Science of the Total Environment 633 (2018) 441–451

Contents lists available at ScienceDirect

Science of the Total Environment

journal homepage: www.elsevier.com/locate/scitotenv

Dynamic ecological observations from satellites inform aerobiology of allergenic grass pollen

Rakhesh Devadas [a], Alfredo R. Huete [a,*], Don Vicendese [b], Bircan Erbas [b], Paul J. Beggs [c], Danielle Medek [d], Simon G. Haberle [e], Rewi M. Newnham [f], Fay H. Johnston [g], Alison K. Jaggard [c], Bradley Campbell [h], Pamela K. Burton [i], Constance H. Katelaris [j], Ed Newbigin [k], Michel Thibaudon [l], Janet M. Davies [m]

[a] Climate Change Cluster, University of Technology Sydney, 15 Broadway, Ultimo, NSW 2007, Australia
[b] School of Psychology and Public Health, La Trobe University, VIC 3086, Australia
[c] Department of Environmental Sciences, Faculty of Science and Engineering, Macquarie University, NSW 2109, Australia
[d] Waitemata District Health Board, Auckland, New Zealand
[e] Department of Archaeology and Natural History, College of Asia and the Pacific, The Australian National University, Acton, ACT 2601, Australia
[f] School of Geography, Environment and Earth Sciences, Victoria University of Wellington, Wellington, New Zealand
[g] The Menzies Institute for Medical Research at the University of Tasmania, Hobart, Tasmania, Australia
[h] School of Agriculture and Food Science, University of Queensland, QLD, Australia
[i] Department of Medicine, Campbelltown, Hospital, NSW, Australia
[j] Campbelltown Hospital and the School of Medicine, Western Sydney University, Macarthur, NSW, Australia
[k] School of Botany, The University of Melbourne, VIC 3010, Australia
[l] European Aerobiology Society, Réseau National de Surveillance Aérobiologique, 11 chemin de la Creuzille, 69690 Brussieu, France
[m] School of Biomedical Sciences, Institute of Health and Biomedical Innovation, Centre for Children's Health Research, Queensland University of Technology, South Brisbane, QLD 4101, Australia

HIGHLIGHTS

- Grass pollen was studied across five sites in Australia and France.
- Study utilised satellite-derived greenness data to inform grass pollen aerobiology.
- Cross-site timing differences were found in greenness phenology and pollen release.
- Generalised additive models predictive of grass pollen across the diverse sites.
- Potential of satellite data to augment short-term pollen forecast models.

GRAPHICAL ABSTRACT

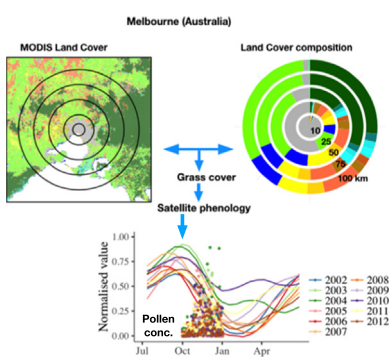

ARTICLE INFO

Article history:
Received 30 September 2017
Received in revised form 16 March 2018
Accepted 17 March 2018
Available online 28 March 2018

ABSTRACT

Allergic diseases, including respiratory conditions of allergic rhinitis (hay fever) and asthma, affect up to 500 million people worldwide. Grass pollen are one major source of aeroallergens globally. Pollen forecast methods are generally site-based and rely on empirical meteorological relationships and/or the use of labour-intensive pollen collection traps that are restricted to sparse sampling locations. The spatial and temporal dynamics of the grass pollen sources themselves, however, have received less attention. Here we utilised a consistent set of MODIS

* Corresponding author at: 15 Broadway, University of Technology Sydney, Ultimo, NSW 2007, Australia.
E-mail addresses: rakhesh.devadas@agriculture.gov.au (R. Devadas), alfredo.huete@uts.edu.au (A.R. Huete), d.vicendese@latrobe.edu.au (D. Vicendese), B.Erbas@latrobe.edu.au (B. Erbas), paul.beggs@mq.edu.au (P.J. Beggs), danielle.medek@waitematadhb.govt.nz (D. Medek), simon.haberle@anu.edu.au (S.G. Haberle), Rewi.Newnham@vuw.ac.nz (R.M. Newnham), Fay.Johnston@utas.edu.au (F.H. Johnston), alison.jaggard@mq.edu.au (A.K. Jaggard), b.campbell2@uq.edu.au (B. Campbell), Pamela.Burton@sswahs.nsw.gov.au (P.K. Burton), connie.katelaris@health.nsw.gov.au (C.H. Katelaris), edwardjn@unimelb.edu.au (E. Newbigin), michel.thibaudon@wanadoo.fr (M. Thibaudon), j36.davies@qut.edu.au (J.M. Davies).

https://doi.org/10.1016/j.scitotenv.2018.03.191
0048-9697/© 2018 Elsevier B.V. All rights reserved.

Editor: Scott Sheridan

Keywords:
Remote sensing
Phenology
Allergic rhinitis
Greenness
Australia
France

satellite measures of grass cover and seasonal greenness (EVI) over five contrasting urban environments, located in Northern (France) and Southern Hemispheres (Australia), to evaluate their utility for predicting airborne grass pollen concentrations. Strongly seasonal and pronounced pollinating periods, synchronous with satellite measures of grass cover greenness, were found at the higher latitude temperate sites in France (46–50° N. Lat.), with peak pollen activity lagging peak greenness, on average by 2–3 weeks. In contrast, the Australian sites (34–38° S. Lat.) displayed pollinating periods that were less synchronous with satellite greenness measures as peak pollen concentrations lagged peak greenness by as much as 4 to 7 weeks. The Australian sites exhibited much higher spatial and inter-annual variations compared to the French sites and at the Sydney site, broader and multiple peaks in both pollen concentrations and greenness data coincided with flowering of more diverse grasses including subtropical species. Utilising generalised additive models (GAMs) we found the satellite greenness data of grass cover areas explained 80–90% of airborne grass pollen concentrations across the three French sites ($p < 0.001$) and accounted for 34 to 76% of grass pollen variations over the two sites in Australia ($p < 0.05$). Our results demonstrate the potential of satellite sensing to augment forecast models of grass pollen aerobiology as a tool to reduce the health and socioeconomic burden of pollen-sensitive allergic diseases.

© 2018 Elsevier B.V. All rights reserved.

1. Introduction

Grass pollen are the most widespread allergens globally with elevated levels of airborne grass pollen linked to increases in hospital emergency department visits and admissions for asthma (Darrow et al., 2012; Erbas et al., 2015). Climate variability, warming temperatures and increased CO_2 levels have been associated with altered flowering times (Fitter and Fitter, 2002), extended pollination periods and increased allergen loads within pollen, thereby increasing human exposure to aeroallergens (Beggs, 2016). The frequency of high pollen concentration days and thunderstorm asthma events are projected to intensify with climate change, further escalating the substantial public health burden of allergic respiratory diseases (Beggs, 2016; Dabrera et al., 2013; Davies et al., 2015).

Management of pollen allergen exposure is an increasingly important public health concern for reducing the health and socio-economic burden of allergic diseases (Beggs et al., 2015; Guillam et al., 2010). Long-term airborne pollen records have been integral towards measuring population exposures in Europe, USA, and other countries, and also provide valuable indicators of current and future trends in allergenic pollen production (Ziello et al., 2012; Ziska et al., 2011). However, conventional methods for sampling airborne pollen utilise volumetric spore collection traps that are labour-intensive, expensive to maintain, and confined to a restrictive range of sampling sites.

Short-term seasonal pollen forecast models have been employed to assist in management of symptoms and disease. These forecast models aim to predict the start of a local pollen season and days of high airborne pollen concentrations utilising meteorological variables (e.g., temperature, relative humidity, wind and precipitation), and may include empirical relationships with airborne pollen concentrations (Laaidi, 2001; Ong et al., 1995; Smith and Emberlin, 2006), as well as local expert knowledge and patients' symptom reports. However, forecast models based on pollen concentration data from one site are not likely to be suitable in other environments (Green et al., 2004). Other observation-based forecasting approaches utilise time series modelling of inter-annual variations in pollen concentrations (Aznarte et al., 2007), meteorological data-driven machine learning and computational intelligence (Voukantsis et al., 2010), and process-based models of chilling requirements (Linkosalo et al., 2008) and photoperiod (García-Mozo et al., 2009).

An important shortcoming in pollen forecasting methods is their lack of utilisation of available ecological information on current land cover conditions, plant species composition (McInnes et al., 2017), and the timing of key plant phenophase periods, such as budburst and flowering. Such data are vital to understand the ecological and climate drivers of pollen aerobiology and may aid the prediction of short-term and future trends of pollen aerobiology. For example, modifications in land cover and land use activities, such as livestock grazing practices, can alter grassland extent, species composition, and flowering phenology, thereby impacting pollen aerobiology in complex ways (Grimm et al., 2008; Rogers et al., 2006; Skjøth et al., 2013).

In the past decade there has been an increase in the availability of satellite remote sensing data of ecologically relevant landscape variables that can augment the restrictive coverage afforded by in situ pollen networks. Satellite data provide timely and repetitive updates of land cover conditions and vegetation phenology status at high spatial resolution (Justice et al., 1998; Zhang et al., 2006). Spatial and temporal analysis using satellite greenness or vegetation indices (VI), have been shown to provide accurate estimates of the onset of birch flowering in Norway (Karlsen et al., 2009), grass and birch flowering in the UK (Khwarahm et al., 2017), the location of grass pollen sources in urban areas in Denmark (Skjøth et al., 2013) and juniper pollen sources in the US (Luvall et al., 2011).

In this study, we investigated the utility of globally consistent satellite remote sensing measures of grass cover and extent and their dynamic phenological growing periods, to inform temporal changes of airborne grass pollen in five contrasting urban environments in the Northern (France) and Southern Hemispheres (Australia). Our aim was to assess the potential of satellite data to augment pollen forecast models and help answer complex questions of changing grass pollen exposure and management of current and future public health threats.

2. Methods

2.1. Site description

Three 'temperate, warm summer, without a dry season' climate sites (Köppen-Geiger Climate Class – Cfb, Peel et al., 2007) in France and two in Australia, with analogous periods of pollen data, were studied (Fig. 1). The sites in France were at higher latitudes (46–50°N) relative to the Australian sites (34–38°S). The two Australian sites and one site in France (Amiens) were coastal and at low elevation (<75 m above sea level), while the other two sites in France were inland with elevations above 175 m.

The two Australian sites had bi-modal seasonal rainfall patterns in contrast to a single summer rainfall season in the three French sites (Fig. 2). Mean annual rainfall (MAR) varied from 634 to 1348 mm and mean annual temperatures (MAT) varied from 10.4 to 17.6 °C. Sydney and Lyon sites had similar and high rainfall (~1300 mm/year), while Melbourne, Montluçon and Amiens had similar and low rainfall (~700 mm/year). All sites had spring seasonal periods of increasing temperatures and vapour pressure deficits (VPD). Wind speeds were high across Austral spring and summer periods in the Australia sites and were high across winter and spring periods in the sites in France (Fig. 2).

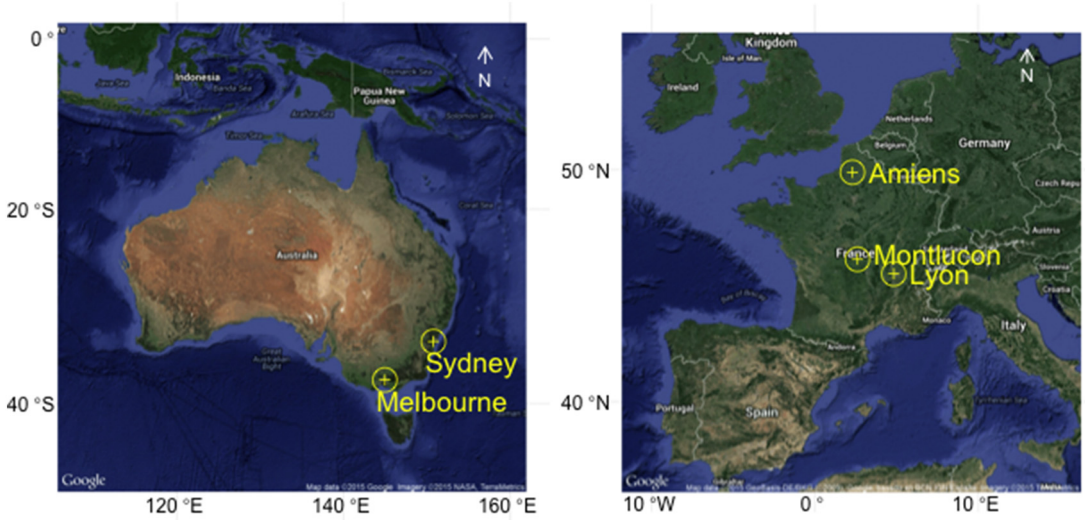

Fig. 1. Two study site locations in Australia (left) and three sites in France (right). Amiens (2.30°E, 49.90°N), Montluçon (2.61°E, 46.34°N), Lyon (4.82°E, 45.72°N), Sydney (150.79°E, 34.07°S), Melbourne (144.96°E, 37.80°S).
Images: Google Earth.

2.2. Pollen data

Daily atmospheric grass pollen concentration data were obtained for the five sites. The pollen data for the 3 sites in France and Melbourne site in Australia were available for an 11-year period from 2002 through to end of 2012, while five years of pollen data were available over the Sydney site in Australia, from 2008 through to end of 2012. Aerobiological monitoring of pollen was conducted with volumetric Burkard spore traps/samplers (Burkard Scientific Ltd, Uxbridge, UK) according to methods described in detail previously (Haberle et al., 2014). Pollen was collected and counted at the French sites according to European standard protocols (European Committee for Standardisation, 2015).

2.3. Land cover data

We used MODerate-resolution Imaging Spectroradiometer (MODIS) Land Cover Type 1 (MCD12Q1)-International Geosphere-Biosphere Programme (IGBP) land cover classification data (Friedl et al., 2010) with a spatial resolution of 500 m for the assessment of pollen emission sources. Data were downloaded from the NASA Land Processes Distributed Active Archive Centre (LP DAAC, http://e4ftl01.cr.usgs.gov/). Land cover information was derived for each year of the study to encompass changes in land cover resulting from urbanisation and shifting land uses. The dataset was re-projected from sinusoidal to Universal Transverse Mercator (UTM) projection to make actual area estimates (Fig. 3a).

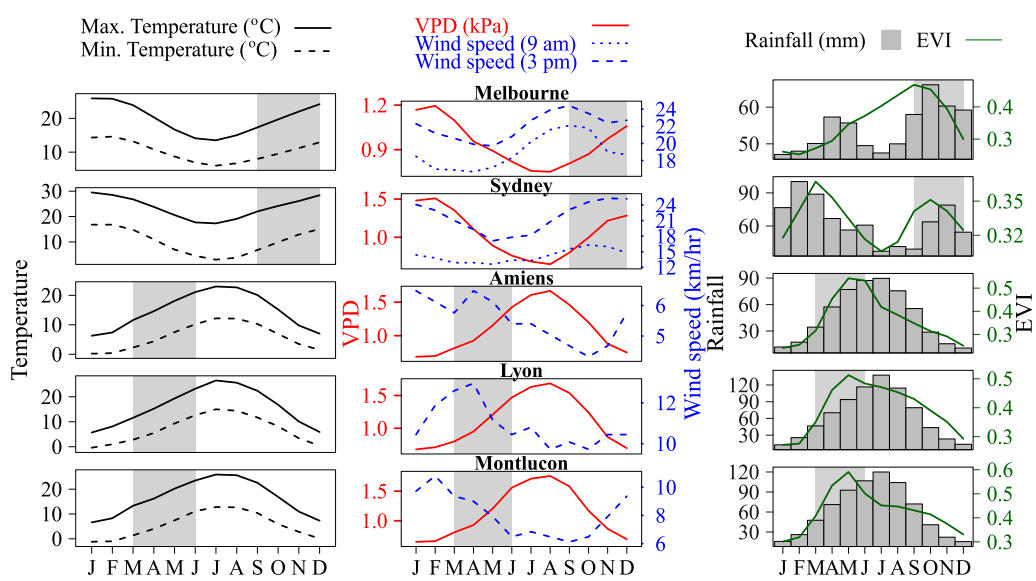

Fig. 2. Long term average monthly maximum, minimum and mean annual temperature (MAT), and mean annual rainfall (MAR) for the 5 study sites. Vapour Pressure Deficit (VPD) data were computed from temperature and relative humidity observations at 3 pm (Allen et al., 1998). Wind speeds were recorded at 3 pm for the French sites, and at 9 am and 3 pm for the coastal, Australian sites. Mean monthly MODIS EVI data were computed over grass-containing land cover classes within the 100 km radius study area. Shaded areas indicate the spring season from September to November in Australia and March to May in France. Australia climate data compiled from Bureau of Meteorology (1971–2014 and 1970–2010 for wind data) http://www.bom.gov.au/climate/averages/maps.shtml; and French sites compiled from U.N. FAO Climate Watch (1971–2000), http://www.fao.org/land-water/databases-and-software/climwat-for-cropwat/en/.

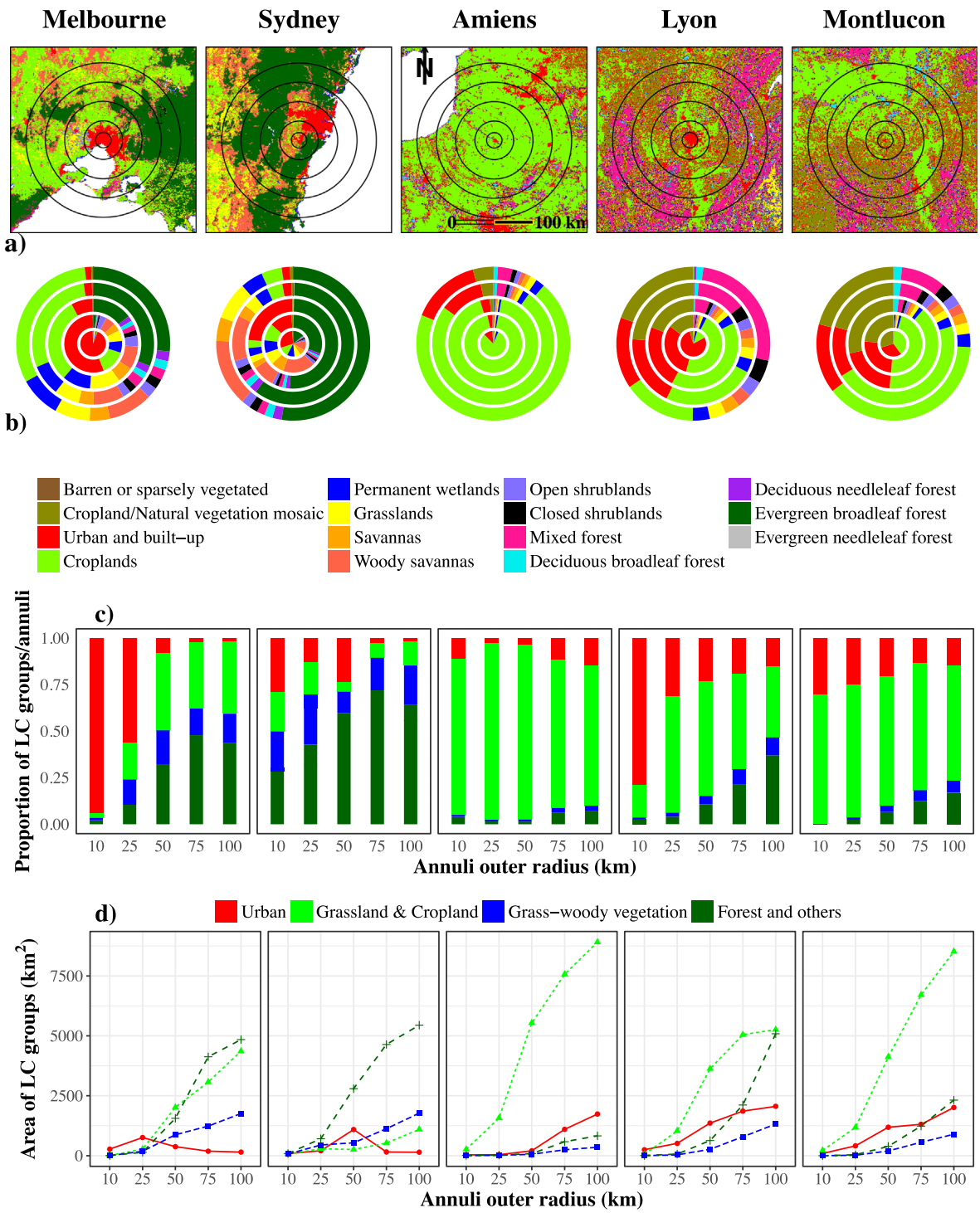

Fig. 3. Land cover for the five urban study areas for the year 2011. (a) MODIS-derived International Geosphere-Biosphere Programme (IGBP) land cover classification with concentric annuli of 0–10 km, 11–25 km, 26–50 km, 51–75 km, and 76–100 km radial distance from pollen sampling source, (b) IGBP land cover class proportions within each of the annuli (note that 0–10 km circle and 11–25 km annulus are not to scale), (c) relative proportions of the 4 composite land cover (LC) classes (urban; grassland & cropland; grass-woody vegetation; forest and others) within each annuli, and (d) actual area of the 4 composite land cover classes in (c) within each annuli.

Regional land cover type data were extracted over a 100 km radius area from the pollen sampler at each of the 5 urban sites. We used a regional (<100 km) definition for pollen transport as presented in Sofiev et al. (2013). These areas were subdivided into (1) sampling circles with radii of 10, 25, 50, 75 and 100 km from the pollen sampler, and (2) sampling annuli at 0–10, 11–25, 26–50, 51–75 and 76–100 km from the pollen sampler (Fig. 3a).

To quantify grass cover across the different IGBP land cover classes, four composite classes were created that included: (1) urban [urban and built-up]; (2) grassland & cropland [grasslands, croplands, and cropland/natural vegetation mosaic]; (3) grass-woody vegetation [savannas, woody savannas, and open shrublands]; and (4) forests and others [all forest and other non-grass classes] (Fig. 3c, d). The first three of these composite classes consisted of seven of the IGBP land cover classes that included significant presence of grass cover, and

were used for further analysis. We included the 'Urban and built-up' class in our grass-containing composite class because urban structures such as parks, golf courses, residential lawns, and other recreational areas, all provide significant 'local sources' of grasses in very close proximity to the pollen traps. The fourth composite class (forests and others) comprised land cover classes without significant presence of grass cover and were masked and not considered in further analysis. The final result of this analysis was a set of 500 m resolution images, derived consistently over all 5 study areas, showing the spatial distribution of potential grass pollen source areas.

2.4. Satellite greenness data

Spatial and temporal changes in grass growth at all sites were determined from the satellite-derived Enhanced Vegetation Index (EVI) product from Terra MODIS sensor (Huete et al., 2002). The EVI was used as a spectral surrogate of vegetation chlorophyll activity and enabled continuous and long-term observations of vegetation seasonal and interannual dynamics on a pixel-by-pixel basis. EVI is computed as,

$$EVI = 2.5\text{x}\frac{NIR - RED}{NIR + 6\,\text{x}\,RED\text{-}7.5\,\text{x}\,Blue + 1} \quad (1)$$

where NIR and RED and Blue are atmospherically corrected surface reflectances in the near-infrared, red and blue wavebands, respectively.

The standard Terra MODIS 16-day composite EVI (MOD13A1) product at 500 m spatial resolution for 2000 to 2014 was downloaded from the NASA LP DAAC. This product has the strictest quality control (QC) measures applied and is optimised to the nominal 16-day repeat orbital cycle of the MODIS sensor (Didan, 2015). The EVI data was filtered based on the quality assurance (QA) flags provided in the product and gap filled using a linear method involving five chronologically arranged datasets (Fensholt and Proud, 2012). Spatially averaged satellite EVI time series data of the composite grass cover classes were compiled by annuli and circles within the 100 km radius circles at each site (Fig. 3c, d).

2.5. Modelling of pollen concentrations

Generalised Additive Models (GAMs) (Hastie and Tibshirani, 1990; James et al., 2013) were used to test the relationships and potential prediction capabilities of grass pollinating periods with the seasonal EVI profiles for all the study sites and grass cover sampling regimes (circle, annuli). GAMs provide a conceptual modelling framework for extending a standard linear model by allowing non-linear functions of explanatory variables, while maintaining additivity (Hastie and Tibshirani, 1990; James et al., 2013). For predicting y using several predictors, x1, x2…xp, GAMs can be represented as,

$$y = b0 + f\,(x1) + f\,(x2) + f\,(x3) + f\,(x4) \quad (2)$$

where, y is 14-day moving average of daily grass pollen concentrations, $b0$ is the intercept, $x1$ is 16 day-lagged EVI, $x2$ is 32 day-lagged EVI, $x3$ is 48 day-lagged EVI and $x4$ is the Julian day.

A 14-day moving average of daily grass pollen concentrations was employed mainly to capture the seasonal variability of pollen concentration. We used three time-lagged EVI data, or 48 days, and Julian day as predictor variables. The pollen concentration on a specific day was thus modelled using previous, lagged EVI observations, so that the GAM models would have the potential to predict pollen concentrations, weeks or even months ahead. In addition to the lagged EVI, Julian day was also included as a predictor variable to capture the general seasonality of pollen generation.

2.6. Model validation

Mean EVI time series data pertaining to the relevant grass cover areas for each circle and annuli sample were generated and separate GAMs were fitted for all the study locations. All EVI data corresponding to available grass pollen data during years 2000–2013 were used for training the GAM models. Prediction capabilities of the models were evaluated with the correlation coefficient (r) between actual and predicted grass pollen concentration and the root mean square error (RMSE). For validation of the prediction capabilities of the GAMs, actual grass pollen concentration data for the most recent pollen season at each site (2013–14 for the Australian sites; and 2014 for the French sites) were used, i.e., this independent data year was not included in the data to generate the GAMs. We used the entire 100 km sampling area at each site to predict daily grass pollen levels for the independent pollen season.

3. Results

3.1. Distribution of grass pollen sources (land cover analysis)

The functional composition of the IGBP land cover classes contrasted distinctly between the Australian and French sites (Fig. 3a, b). Whereas the French sites were relatively homogeneous with primarily herbaceous (grass and cereal crop) cover, the Australian sites (Melbourne and Sydney) were distinctly heterogeneous in grass and forest vegetation. Substantial grass cover with potential to be emission sources of grass pollen was found in all study areas. However, there were significant differences in the proportions of the different land cover classes across the five study sites (Fig. 3). Almost half (49%) of the total area at the Melbourne site was comprised of grass-containing land cover classes (composited groups 1–3), whereas the grass vegetated land cover classes accounted for only 25% of the total area for Sydney. Grassland vegetation made up significant proportions of the total peri-urban area for the French sites, with 88% (Amiens), 75% (Lyon), and 87% (Montluçon).

Forests were primarily present in the peri-urban, >50 km annuli at the Australian sites and in the outermost 76–100 km annulus in Lyon, France. The surrounds of the Sydney site largely consisted of evergreen broadleaf forests (Eucalyptus open forests) ranging from 25 to 75% of total area across the annuli (Fig. 3c, d). Urban class area within the 100 km circle was substantially higher for the French sites (Amiens – 10%, Lyon – 19% and Montluçon – 16%) compared to Australian sites (Melbourne – 6% and Sydney – 5%). The relative proportion of the urban class within each annulus decreased with distance from the trap in Melbourne, Lyon, and Montluçon, and was particularly high in the 0–10 km annulus in Melbourne and Lyon (Fig. 3c). Actual area of the urban class was highest near the pollen trap location in Melbourne (11–25 km annulus), while in Sydney the maximum urban class area occurred within the 25–50 km annulus, primarily a result of the pollen trap location outside the centre of the city (Fig. 3d). Urban land class area increased with distance from the pollen trap locations in Lyon, Montluçon, and Amiens.

3.2. Comparison of EVI and grass pollen concentration time series data

The multiple year airborne grass pollen concentrations are plotted alongside the satellite EVI time series data for the grass covered areas at various distances (annuli) from the grass pollen sampler in Fig. 4. At the French sites seasonal airborne pollen concentrations corresponded well with satellite EVI data of the grass cover seasonal profiles, with peak grass activity (greenness) and pollen concentrations occurring during the warm late spring and early summer months (May–June) and dormant grass (minimal greenness) with no airborne grass pollen during the cold winter periods (January–February). Satellite-derived grass cover greenness values varied only slightly across the various

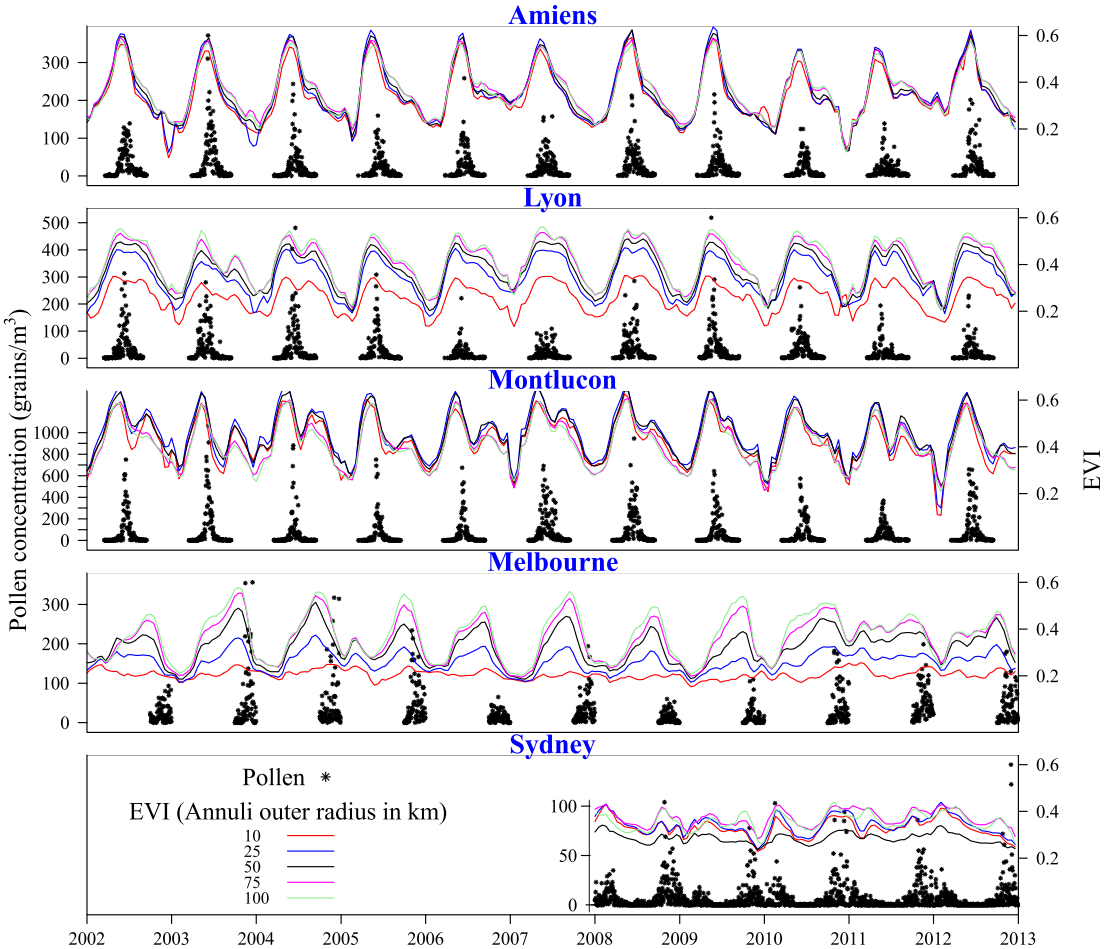

Fig. 4. Time series plots of grass pollen concentrations and MODIS satellite EVI for the composite grass-containing land cover classes in each annuli for the French and Melbourne sites (2002—2012) and Sydney (2008–2012) site. Note that grass pollen data for Melbourne is only available for a 3 months period (Oct–Dec).

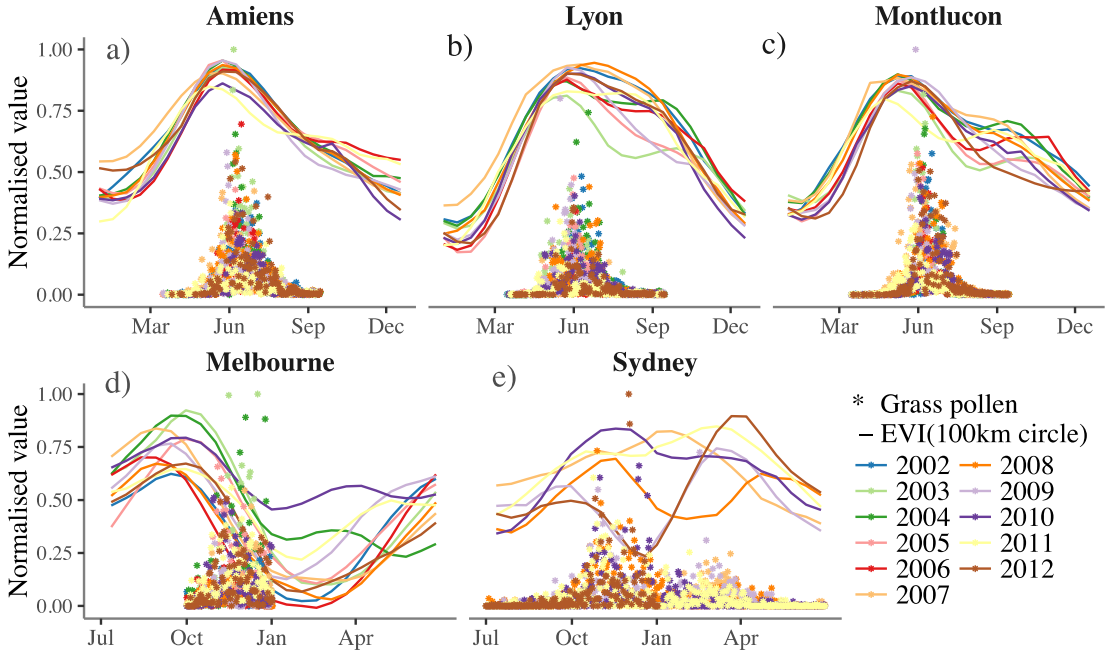

Fig. 5. Stacked, multi-annual grass pollen concentration and satellite-derived EVI seasonality for the grass containing land cover classes within the 100 km composite circle at France and Australian sites. Grass pollen concentration and EVI values were normalised (0–1) based on their maximum and minimum values. The year from July–June was used for Australia to centre summer in both plots. Note that grass pollen data for Melbourne is only available for a 3 months period (Oct–Dec).

annuli of increasing distance from the pollen sampler, with the exception of the highly urbanised area (0–10 km annulus) in Lyon, which had much lower EVI values (Fig. 4). The small differences in satellite EVI time series profiles across annuli reflected minor variations in the extent of grass cover and their phenological timing (Fig. 3a, c).

In contrast, Melbourne exhibited more spatially variable grass cover growth patterns with distance from the pollen sampler. Grass cover EVI values and seasonality were strongest at the greatest distance annulus (76–100 km) and decreased with proximity to the urban pollen sampler, which showed low and seasonally weak EVI over the urbanised, 0–10 km annulus area (Fig. 4). The airborne grass pollen peak concentrations at the Melbourne site significantly lagged satellite EVI peaks across all annuli, irrespective of the distance from the pollen sampler (Fig. 4). The Sydney site showed more complex grass cover greening and grass pollen concentration dynamics, with airborne grass pollen concentrations and grass cover growth continuously active throughout the year (Fig. 4), primarily as a result of the milder Sydney climate (Fig. 2). Secondary peaks in grass cover greenness and grass pollen concentrations were also observed (Fig. 4).

Normalised values of airborne grass pollen concentrations and satellite EVI for all spatially distributed grass cover areas within the entire 100 km study area were stacked by individual year to compare pollen with EVI phenological variations at each of the five sites (Fig. 5). The French sites showed strong synchronous patterns in both grass pollen concentration and EVI data with little inter-annual variability in either the grass pollen or the EVI data. Spring season increases in grass pollen concentrations were preceded by a sustained increase in EVI with peak EVI values observed approximately 11, 19, and 21 days, on average, in advance of peak grass pollen concentrations over Amiens, Lyon, and Montluçon, respectively (Fig. 5).

The satellite EVI and grass pollen phenology profiles exhibited much stronger inter-annual variability at the Australian sites compared with the French sites (Fig. 5). At the Melbourne site EVI peaks (typically September) were, on average, 52 days in advance of peak grass pollen concentrations in late Austral spring (November). The Sydney site also had a strong pollen release period in November, but also showed a secondary pollen period in Austral autumn (March) (Fig. 5). These bi-modal peaks in grass pollen concentrations at the Sydney site corresponded with bi-modal rainfall and EVI peaks (Fig. 2), although the relative dominance and timing of spring and autumn EVI peaks varied considerably from year to year, and in some years (e.g. 2010/11 and 2011/12), the two grass pollen periods merged, resulting in one continuous grass pollen season extending from spring to autumn (Fig. 5). In Sydney, the average Austral spring seasonal peak in grass pollen concentration (November) lagged behind satellite EVI peaks (October) by 30 days.

3.3. Modelling and prediction of pollen concentration in a GAM framework

The prediction capability of the general additive models (GAM) generally varied among sites and across annuli and composite circle areas (Fig. 6 and Fig. 3a, b). The model prediction outcomes for the independent grass pollen season test (2014 for France and 2013/14 for Australia) were far more accurate over the French sites compared with the Australian sites, as shown by the higher correlation coefficients ($r > 0.90$, p-value < 0.001) and lower root mean square error (RMSE) (between 5 and 10%).

At the French sites, GAM-based predictive capabilities did not vary markedly across individual annuli and composite area EVI sampling regimes, indicative of the relatively homogeneous land cover conditions. A slight increase in correlation coefficient and decrease in RMSE were observed for Montluçon at samplings (annuli and area) beyond 25 km from the pollen sampler. For the most part, EVI data from the broadly distributed grass cover at the French sites (100 km radius study area) yielded daily grass pollen predictions explaining between 80 and 90% of the variance ($p < 0.001$) and the slowest RMSE, although at the Amiens site, the highly local, 0–10 km circle yielded the lowest RMSE values (Fig. 6).

At the Australian sites, a wider range of correlative predictions of the grass pollen season (r increasing from 0.6 to 0.9) was found across the annuli and composite sampling areas (Fig. 6). At the Melbourne site, model predictions were more accurate beyond the 50 km annuli and

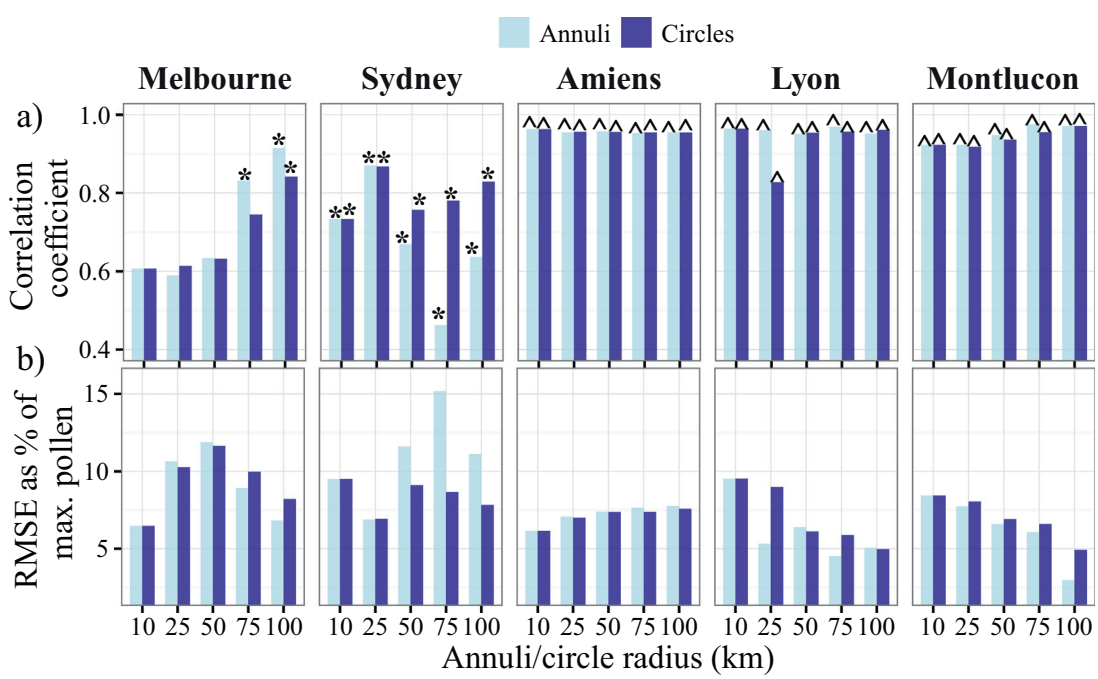

Fig. 6. General additive model predictions of daily levels of airborne grass pollen at the pollen sampler for each site, using EVI values of distributed grass cover within each annulus and circle at each site. (a) Correlation coefficients between the actual and predicted (modelled) atmospheric grass pollen concentration over the 2013/14 Australian pollen season and 2014 French pollen season (statistically significant correlations, $^*p < 0.05$ and $^\wedge p < 0.001$); (b) Root mean square error (RMSE) of correlation coefficients as a percentage of the maximum grass pollen concentration.

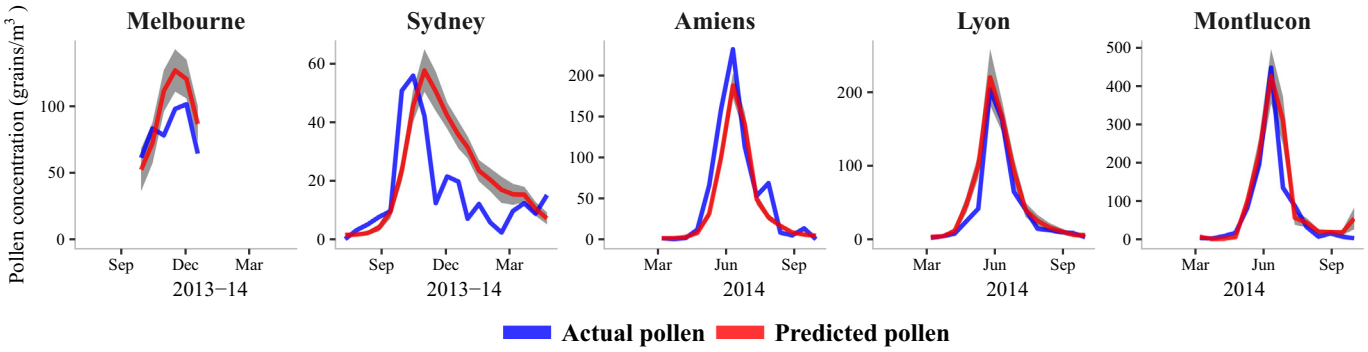

Fig. 7. Comparisons of GAM model-generated pollen seasonality with actual pollen data for the independent pollen seasons (2013–14 pollen season for 2 Australian sites and 2014 pollen season for 3 French sites). Mean EVI values for site-specific sampling areas over three time lags (16, 32 and 48 days), along with Julian day were used as the predictor variables. The GAM model was based on distributed grass cover EVI over the composite 100 km radius sampling area for sites. Grey area is 95% confidence interval.

composite study areas from the pollen sampler ($p < 0.05$), as grass cover proportions increased with distance from the pollen sampler (Fig. 3c). In the case of Sydney, the sampling annuli and circles explained 74% to 79% of the variance ($p < 0.05$), with prediction accuracies highest in the 0–25 km circle ($r = 0.87$) and 11–25 km annuli ($r = 0.87$) samples, both with the lowest RMSE (7%). These sampling areas occurred between the relatively low urban cover location of the pollen sampler and the highly urbanised inner Sydney city area 40 km away (Fig. 3a). The next best GAM model result was when distributed grass cover was sampled from the entire 100 km composite area ($r = 0.83$, Fig. 6).

The GAM-generated seasonal profile prediction of grass pollen concentrations for the independent pollen season is shown in Fig. 7 for distributed grass cover within the 100 km composite study area. The predicted seasonal pollen profiles, peak timing and magnitudes, compared well with actual grass pollen levels at all three French sites. In contrast, the seasonal timing of pollen peaks and magnitudes of grass pollen concentrations were less well predicted at the Australian sites. At the Sydney site, predicted pollen peak timing lagged the actual peak pollen by a few weeks, while at the Melbourne site predicted peak pollen was one month in advance of the actual peak pollen period (Fig. 7). At both sites, predicted pollen exceeded actual pollen levels through most of the pollen season.

4. Discussion

This study exemplifies the potential for remote sensing imagery to augment the geographic coverage and effectiveness of seasonal forecasts of grass pollen exposure in temperate regions to improve clinical and patient self-management of allergic diseases. The satellite data contributed both important geospatial landscape information on local and regional grass pollen emission sources and the timing of key phenology growth periods. Using grass pollen concentrations with Julian day and three, 16-day lags of satellite greenness data in a GAM framework, we were able to explain aerobiological pollen variations across the five sites studied here, although with coefficients of determination that were quiet variable, R^2 ranging from 0.34 to 0.90. Seasonal pollen variations over the 3 sites in France showed clear phenology profiles and were best modelled with the satellite data (R^2 from 0.84 to 0.90). In contrast, satellite data only accounted for 34% and 78% of the seasonal variation in pollen concentrations at the Australian Melbourne and Sydney sites, respectively, partly due to the more heterogeneous landscape mosaics, but also suggesting other explanatory variables (e.g. wind vector data), not captured in the satellite EVI product, are needed to enable effective monthly and weekly predictive models for forecasting the timing and magnitude of atmospheric grass pollen.

Satellite greenness monitoring revealed landscape process information of grass cover phenology, a fundamental ecological plant trait that integrates local climate, soils, land use, and disturbance factors (Cleland et al., 2007; Richardson et al., 2013). Previous studies have used satellite data to inventory grass pollen sources, as for example, over the city of Aarhus, Denmark (Skjøth et al., 2013). In a UK study, Khwarahm et al. (2017) used a total chlorophyll index from the MERIS satellite, MTCI, to predict the onset of birch tree and grass flowering periods, which corresponded to the timing of pollen release. This study was the first to attempt to compare Southern and Northern Hemisphere sites and relate the phenology of Australian grassland dynamics with grass seasonal pollen release activity. Using a globally consistent set of satellite data, our results showed significant differences in the relationships between grass cover satellite phenology and pollen release periods both within and across the French and Australian sites, with seasonal pollen activity lagging behind seasonal satellite greenness from 2 to 7 weeks over the studied sites.

Landscape conditions and climate may be partly responsible for the contrasting results between the French and Australian sites. Land cover types and grass species at the French sites were relatively homogeneous and uniformly distributed, resulting in well-defined and sharp (narrow) phenology profiles. The dominant plant species over the three French sites included a major presence of agricultural crops (e.g., colza and wheat) along with temperate grassland meadows and cultivated grassland fodder. Land cover conditions and grass cover phenology profiles at the Australian sites were more heterogeneous and comprised diverse grass species, yielding broader phenology profiles. In the Melbourne site, grass diversity was dominated by temperate or spring-flowering species (Davies et al., 2015), while in the Sydney region, grass cover areas consist of native and exotic species, as well as the co-existence of mixed temperate cool-season grasses (C_3 species) and subtropical or summer-flowering grasses (C_4 species) (Davies et al., 2015; Medek et al., 2016). It is likely that these functionally diverse grasses, each with contrasting growth requirements, contributed to year-round grass flowering and multiple peaks of airborne grass pollen and satellite greenness (Medek et al., 2016). Grass phenological diversity may also partly explain the cross-site differences in observed lags between EVI and the pollen concentration time series data.

Seasonal and inter-annual variability were also much greater at the Australian sites compared with the sites in France. Beggs et al. (2015) reported "striking spatial and temporal variability in grass pollen seasons in Australia", with important implications for the Australian grass pollen-allergy community. Grasslands are among the most vulnerable and ecologically sensitive biomes to climate variability and are particularly susceptible to species invasions and shifts in species diversity (Moran et al., 2014; Seddon et al., 2016). Notably, most allergenic grass species are not endemic to Australia. Warm season C_4 grasses are expected to expand into cooler temperate areas with continued climate warming, which could be problematic, considering that current allergen-specific immunotherapy treatments may not effectively cover subtropical grass pollen allergens (Nony et al., 2015). Such inter-annual variations will need to be more thoroughly considered in the evaluation of robust GAM model performance.

We have demonstrated that land cover distribution and distance influence the relation of pollen emission sources with airborne grass pollen concentrations at target "sink" locations of interest (e.g., human populated areas), particularly at the Australian sites with higher vegetation heterogeneity. This suggests land cover changes associated with urban expansion and peri-urban land use activities induce changes in pollen aerobiology by altering the location, amounts, and timing of emission sources with potential climate interactions. Nevertheless, despite the complex landscape conditions, this study has shown that satellite greenness data can function effectively in monitoring and tracing grass pollen aerobiology. Given the highly dynamic nature of land cover status and condition, remote sensing thus provides a powerful public health tool because of its synoptic coverage and monitoring capabilities that can be used to augment predictive models of major aeroallergen exposures within populated urban and surrounding areas.

Potential advances in pollen predictions can be made through improved assessments of grass pollen emission source mapping, particularly in diverse landscapes in which mixtures of vegetation functional groupings (grass, shrub, tree) and species composition are poorly resolved and are not well represented in existing land cover classifications. The IGBP 'built-up urban' land cover class designation provides no information on grass cover, yet urban 'green spaces' play a significant role in grass pollen exposure to the public given the proximity factor (Skjøth et al., 2013). Finer scale land cover maps would improve upon the mapping of grass cover sources (e.g. parks, golf courses, lawns), although they would be based on local or regional methods (e.g. Urban Atlas), updated less frequently, and not globally consistent. Finer spatial resolution Landsat and Sentinel-2 satellite data offer 10–30 m pixel resolution, globally consistent data that can better resolve grass cover areas and urban green spaces, and offer the potential of generating more precise and updated land cover maps (Chen et al., 2015).

Prior to implementation of satellite-based pollen forecasting, the optimal temporal frequency of satellite data may need to be investigated. Standard MODIS vegetation index products and phenology products are available at 16-day composited periods so that clouds can be effectively masked and removed, atmosphere contaminants (e.g., aerosols) minimised, and variations in sensor view geometries corrected for. Nevertheless, reducing the window over which satellite data is sampled would better define key phenophase periods and the lags between peak EVI and peak pollen activity observed in this study over the different locations. Thus, further studies are needed to assess whether higher frequency satellite data, including daily data can improve upon phenology parameter retrievals and forecasting of the pollen season.

The lower significance of the GAM's for Melbourne and Sydney highlights the need for further research to understand additional factors that may be required to inform an accurate operational pollen forecast system with truly synoptic coverage. In this cross-site modelling study, we only assessed the prediction of a single spring pollen season (austral spring in Australia), and did not attempt to predict multiple pollen seasons, as seen with the smaller autumn pollen season at the Sydney site. Thus, our GAM model missed the second pollen peak in Sydney and this may justify additional lags in the GAM model to capture multiple or year-round flowering seasons. The contribution of other parameters not captured in the satellite phenology signal, such as wind direction, wind speed, temperature and vapour pressure deficit, to satellite-informed pollen forecast models need to be further evaluated.

There are important meteorological influences and interactions that must be considered in coupling satellite information on geo-locational grass pollen sources with measured pollen concentrations at pollen traps. At our five study sites, wind speeds were highest during the active pollen season, an evolutionary adaptation of wind-pollinated grass species that couple local site meteorological conditions with phenological flowering states, and pollen concentrations in the atmosphere. Wind vector data will further vary hourly and daily, and a pollen forecasting model will need to ingest wind vector information to drive it at the needed time scales.

At the two Australian coastal sites, wind speeds varied significantly with time of day, with more intense wind speeds at 3 pm relative to the calmer wind speeds at 9 am, year-round (Fig. 2). In Sydney, where the grass pollen season was somewhat bimodal, wind speeds were high for both pollen peaks, although slightly stronger during the dominant austral spring pollen peak, compared with the weaker austral autumn pollen peak. Afternoon sea breezes were also >50% stronger than morning land breezes during both austral spring and autumn grass pollen peaks, and only the land breezes would primarily contribute pollen to the atmosphere. In Melbourne the peak wind speeds coincided with the start of the austral spring pollen season (Sep–Oct). In contrast to Sydney, Melbourne morning land breezes persisted into the afternoon, although sea breezes were equally significant in the afternoon.

Thus, meteorological factors and influences on pollen were quite varied even between the two Australian sites. By contrast, the more continental French sites were dominated by larger-scale synoptic conditions and topographic effects. The role of meteorological factors thus need further attention as contributory drivers for the cross-site variability in pollen-satellite relationships observed in this study. If GAM-based predictions are to be made across sites or if differences in GAM results are to be explained within sites, then meteorological factors will have to be included. Other factors to be considered, which may also not be captured by the satellite greenness signal include, soil moisture, relative humidity, and air temperatures.

A comprehensive or robust pollen forecasting model would require better knowledge of pollen source sampling patterns. Pollen trap source footprints and local to regional scale relationships do not appear to be well understood for grasses. Grass pollen studies generally limit sampling distances to within 50 km from the pollen trap, however, we found some GAM prediction improvements when extending the sampling to 100 km distances. Aylor et al. (2006) noted that the impact of pollen may extend to greater distances because dispersal distributions typically have long extending tails, especially for large source areas, and the bi-weekly temporal scale of this study along with pollen retransport possibilities across multiple meteorologically-conducive days may have enabled dispersal contributions from >50 km distances. In summary, a better characterization of the pollen trap grass source footprint is needed, weighted by wind and other meteorological factors, to improve upon grass pollen forecast models. If the potential of EVI to inform pollen forecast systems were realised, then the significant resources utilised for local labour-intensive pollen monitoring networks could be substantially reduced.

5. Conclusions

The satellite EVI greenness signal used here encapsulates in a timely fashion a range of environmental variables within the one phenology measure, including the influence of local soil condition, land cover diversity, and meteorology on airborne pollen concentrations at weekly scales. Nevertheless, daily operational and weekly predictive pollen forecast models are likely to require integration of EVI data with meteorological data (e.g. wind) and to be validated by pollen monitoring. We provide herein evidence of the utility of remote sensing to contribute information on land cover and phenology conditions to advance the capability for short-term forecasting of peaks in the level and timing of airborne grass pollen with wide synoptic coverage to assist in clinical and public health management of the grass pollen allergen exposure risks.

Funding sources

The Australian Aerobiology Working Group was supported by a grant from the Australian Centre for Ecological Analysis and Synthesis (ACEAS) as part of the Australian Terrestrial Ecosystem Research Network (TERN). Merck Sharp and Dohme provided additional

independent untied co-sponsorship for the Working Group. This research has received ongoing financial support from the Australasian Foundation for Immunology and Allergy, Asthma Australia and Stallergenes Australia Pty Ltd through the Australian Pollen Allergen Partnership; and through an Australian Research Council award, DP170101630 - Satellite Tracking of Emerging Health Threats from Grass Pollen Exposure.

Acknowledgements

This work was an outcome of the second workshop (November 2013) of the Australian Aerobiology Working Group. The authors wish to thank Associate Professor Alison Specht and the staff of ACEAS and TERN for assistance in organising the Australian Aerobiology Workshops "Understanding Australian aerobiology to monitor environmental change and human allergenic exposure", North Stradbroke Island, Australia.

References

Allen, R.G., Pereira, L.S., Raes, D., Smith, M., 1998. Crop Evapotranspiration: Guidelines for Computing Crop Water Requirements - FAO Irrigation and Drainage Paper 56. FAO - Food and Agriculture Organization of the United Nations, Rome.

Aylor, D.E., Boehm, M.T., Shields, E.J., 2006. Quantifying aerial concentrations of maize pollen in the atmospheric surface layer using remote-piloted airplanes and lagrangian stochastic modeling. J. Appl. Meteorol. Climatol. 45:1003–1015. https://doi.org/10.1175/jam2381.1.

Aznarte, M.J.L., Benítez Sánchez, J.M., Lugilde, D.N., de Linares Fernández, C., de la Guardia, C.D., Sánchez, F.A., 2007. Forecasting airborne pollen concentration time series with neural and neuro-fuzzy models. Expert Syst. Appl. 32:1218–1225. https://doi.org/10.1016/j.eswa.2006.02.011.

Beggs, P.J. (Ed.), 2016. Impacts of Climate Change on Allergens and Allergic Diseases. Cambridge University Press, Cambridge.

Beggs, P.J., Katelaris, C.H., Medek, D., Johnston, F.H., Burton, P.K., Campbell, B., et al., 2015. Differences in grass pollen allergen exposure across Australia. Aust. N. Z. J. Public Health 39:51–55. https://doi.org/10.1111/1753-6405.12325.

Chen, J., Chen, J., Liao, A., Cao, X., Chen, L., Chen, X., et al., 2015. Global land cover mapping at 30 m resolution: a POK-based operational approach. ISPRS J. Photogramm. Remote Sens. 103:7–27. https://doi.org/10.1016/j.isprsjprs.2014.09.002.

Cleland, E.E., Chuine, I., Menzel, A., Mooney, H.A., Schwartz, M.D., 2007. Shifting plant phenology in response to global change. Trends Ecol. Evol. 22:357–365. https://doi.org/10.1016/j.tree.2007.04.003.

Dabrera, G., Murray, V., Emberlin, J., Ayres, J.G., Collier, C., Clewlow, Y., et al., 2013. Thunderstorm asthma: an overview of the evidence base and implications for public health advice. QJM 106:207–217. https://doi.org/10.1093/qjmed/hcs234.

Darrow, L.A., Hess, J., Rogers, C.A., Tolbert, P.E., Klein, M., Sarnat, S.E., 2012. Ambient pollen concentrations and emergency department visits for asthma and wheeze. J. Allergy Clin. Immunol. 130:630–638.e4. https://doi.org/10.1016/j.jaci.2012.06.020.

Davies, J.M., Beggs, P.J., Medek, D.E., Newnham, R.M., Erbas, B., Thibaudon, M., et al., 2015. Trans-disciplinary research in synthesis of grass pollen aerobiology and its importance for respiratory health in Australasia. Sci. Total Environ. 534:85–96. https://doi.org/10.1016/j.scitotenv.2015.04.001.

Didan, K., 2015. MOD13A3 MODIS/Terra Vegetation Indices Monthly L3 Global 1 km SIN Grid V006 [Data Set]. NASA EOSDIS LP DAAC. https://doi.org/10.5067/MODIS/MOD13A3.006.

Erbas, B., Dharmage, S.C., Tang, M.L.K., Akram, M., Allen, K.J., Vicendese, D., et al., 2015. Do human rhinovirus infections and food allergy modify grass pollen-induced asthma hospital admissions in children? J. Allergy Clin. Immunol. 136:1118–1120.e2. https://doi.org/10.1016/j.jaci.2015.04.030.

European Committee for Standardisation, 2015. Ambient Air - Sampling and Analysis of Airborne Pollen Grains and Fungal Spores for Allergy Networks - Volumetric Hirst Method [English Version] Technical Specification CEN/TS 16868.

Fensholt, R., Proud, S.R., 2012. Evaluation of earth observation based global long term vegetation trends — comparing GIMMS and MODIS global NDVI time series. Remote Sens. Environ. 119:131–147. https://doi.org/10.1016/j.rse.2011.12.015.

Fitter, A.H., Fitter, R.S.R., 2002. Rapid changes in flowering time in British plants. Science 296:1689–1691. https://doi.org/10.1126/science.1071617.

Friedl, M.A., Sulla-Menashe, D., Tan, B., Schneider, A., Ramankutty, N., Sibley, A., Huang, X., 2010. MODIS collection 5 global land cover: algorithm refinements and characterization of new datasets. Remote Sens. Environ. 114:168–182. https://doi.org/10.1016/j.rse.2009.08.016.

García-Mozo, H., Galán, C., Belmonte, J., Bermejo, D., Candau, P., Díaz de la Guardia, C., et al., 2009. Predicting the start and peak dates of the Poaceae pollen season in Spain using process-based models. Agric. For. Meteorol. 149:256–262. https://doi.org/10.1016/j.agrformet.2008.08.013.

Green, B.J., Dettmann, M., Yli-Panula, E., Rutherford, S., Simpson, R., 2004. Atmospheric Poaceae pollen frequencies and associations with meteorological parameters in Brisbane, Australia: a 5-year record, 1994-1999. Int. J. Biometeorol. 48:172–178. https://doi.org/10.1007/s00484-004-0204-8.

Grimm, N.B., Faeth, S.H., Golubiewski, N.E., Redman, C.L., Wu, J., Bai, X., et al., 2008. Global change and the ecology of cities. Science 319:756–760. https://doi.org/10.1126/science.1150195.

Guillam, M.T., Antoine, L.C., Chevallier, D., Dubreil, Y., Figureau, C., Morin, O., et al., 2010. Prevention of pollinosis: study of an intervention providing information and advice to begin treatment. Rev. Fr. Allergol. 50:493–500. https://doi.org/10.1016/j.reval.2010.02.016.

Haberle, S.G., Bowman, D.M.J.S., Newnham, R.M., Johnston, F.H., Beggs, P.J., Buters, J., et al., 2014. The macroecology of airborne pollen in Australian and New Zealand urban areas. PLoS One 9, e97925. https://doi.org/10.1371/journal.pone.0097925.

Hastie, T.J., Tibshirani, R.J., 1990. Generalized Additive Models. Chapman and Hall/CRC, Boca Raton.

Huete, A., Didan, K., Miura, T., Rodriguez, E.P., Gao, X., Ferreira, L.G., 2002. Overview of the radiometric and biophysical performance of the MODIS vegetation indices. Remote Sens. Environ. 83:195–213. https://doi.org/10.1016/s0034-4257(02)00096-2.

James, G., Witten, D., Hastie, T., Tibshirani, R., 2013. An Introduction to Statistical Learning With Applications in R. Springer, New York.

Justice, C.O., Vermote, E., Townshend, J.R.G., Defries, R., Roy, D.P., Hall, D.K., et al., 1998. The moderate resolution imaging spectroradiometer (MODIS): land remote sensing for global change research. IEEE Trans. Geosci. Remote Sens. 36:1228–1249. https://doi.org/10.1109/36.701075.

Karlsen, S.R., Ramfjord, H., Høgda, K.A., Johansen, B., Danks, F.S., Brobakk, T.E., 2009. A satellite-based map of onset of birch (*Betula*) flowering in Norway. Aerobiologia 25:15–25. https://doi.org/10.1007/s10453-008-9105-3.

Khwarahm, N.R., Dash, J., Skjøth, C.A., Newnham, R.M., Adams-Groom, B., Head, K., et al., 2017. Mapping the birch and grass pollen seasons in the UK using satellite sensor time-series. Sci. Total Environ. 578:586–600. https://doi.org/10.1016/j.scitotenv.2016.11.004.

Laaidi, M., 2001. Forecasting the start of the pollen season of Poaceæ: evaluation of some methods based on meteorological factors. Int. J. Biometeorol. 45:1–7. https://doi.org/10.1007/s004840000079.

Linkosalo, T., Lappalainen, H.K., Hari, P., 2008. A comparison of phenological models of leaf bud burst and flowering of boreal trees using independent observations. Tree Physiol. 28:1873–1882. https://doi.org/10.1093/treephys/28.12.1873.

Luvall, J.C., Sprigg, W., Levetin, E., Huete, A., Nickovic, S., Pejanovic, G., et al., 2011. Use of MODIS satellite images and an atmospheric dust transport model to evaluate Juniperus spp. pollen phenology and dispersal to support public health alerts. J. Allergy Clin. Immunol. 127:AB19. https://doi.org/10.1016/j.jaci.2010.12.086.

McInnes, R.N., Hemming, D., Burgess, P., Lyndsay, D., Osborne, N.J., Skjøth, C.A., et al., 2017. Mapping allergenic pollen vegetation in UK to study environmental exposure and human health. Sci. Total Environ. 599–600:483–499. https://doi.org/10.1016/j.scitotenv.2017.04.136.

Medek, D.E., Beggs, P.J., Erbas, B., Jaggard, A.K., Campbell, B.C., Vicendese, D., et al., 2016. Regional and seasonal variation in airborne grass pollen levels between cities of Australia and New Zealand. Aerobiologia 32:289–302. https://doi.org/10.1007/s10453-015-9399-x.

Moran, M.S., Ponce-Campos, G.E., Huete, A., McClaran, M.P., Zhang, Y., Hamerlynck, E.P., et al., 2014. Functional response of U.S. grasslands to the early 21st-century drought. Ecology 95:2121–2133. https://doi.org/10.1890/13-1687.1.

Nony, E., Timbrell, V., Hrabina, M., Boutron, M., Solley, G., Moingeon, P., et al., 2015. Specific IgE recognition of pollen allergens from subtropic grasses in patients from the subtropics. Ann Allergy Asthma Immunol 114:214–220.e2. https://doi.org/10.1016/j.anai.2014.12.005.

Ong, E.K., Singh, M.B., Knox, R.B., 1995. Grass pollen in the atmosphere of Melbourne: seasonal distribution over nine years. Grana 34:58–63. https://doi.org/10.1080/00173139509429034.

Peel, M.C., Finlayson, B.L., McMahon, T.A., 2007. Updated world map of the Köppen-Geiger climate classification. Hydrol. Earth Syst. Sci. 11:1633–1644. https://doi.org/10.5194/hess-11-1633-2007.

Richardson, A.D., Keenan, T.F., Migliavacca, M., Ryu, Y., Sonnentag, O., Toomey, M., 2013. Climate change, phenology, and phenological control of vegetation feedbacks to the climate system. Agric. For. Meteorol. 169:156–173. https://doi.org/10.1016/j.agrformet.2012.09.012.

Rogers, C.A., Wayne, P.M., Macklin, E.A., Muilenberg, M.L., Wagner, C.J., Epstein, P.R., et al., 2006. Interaction of the onset of spring and elevated atmospheric CO_2 on ragweed (*Ambrosia artemisiifolia* L.) pollen production. Environ. Health Perspect. 114:865–869. https://doi.org/10.1289/ehp.8549.

Seddon, A.W.R., Macias-Fauria, M., Long, P.R., Benz, D., Willis, K.J., 2016. Sensitivity of global terrestrial ecosystems to climate variability. Nature 531:229–232. https://doi.org/10.1038/nature16986.

Skjøth, C.A., Ørby, P.V., Becker, T., Geels, C., Schlünssen, V., Sigsgaard, T., et al., 2013. Identifying urban sources as cause of elevated grass pollen concentrations using GIS and remote sensing. Biogeosciences 10:541–554. https://doi.org/10.5194/bg-10-541-2013.

Smith, M., Emberlin, J., 2006. A 30-day-ahead forecast model for grass pollen in north London, United Kingdom. Int. J. Biometeorol. 50:233–242. https://doi.org/10.1007/s00484-005-0010-y.

Sofiev, M., Belmonte, J., Gehrig, R., Izquierdo, R., Smith, M., Dahl, Å., Siljamo, P., 2013. Airborne pollen transport. In: Sofiev, M., Bergmann, K.-C. (Eds.), Allergenic Pollen: A Review of the Production, Release, Distribution and Health Impacts. Springer, Dordrecht:pp. 127–159 https://doi.org/10.1007/978-94-007-4881-1.

Voukantsis, D., Niska, H., Karatzas, K., Riga, M., Damialis, A., Vokou, D., 2010. Forecasting daily pollen concentrations using data-driven modeling methods in Thessaloniki, Greece. Atmos. Environ. 44:5101–5111. https://doi.org/10.1016/j.atmosenv.2010.09.006.

Zhang, X., Friedl, M.A., Schaaf, C.B., 2006. Global vegetation phenology from moderate resolution imaging Spectroradiometer (MODIS): evaluation of global patterns and comparison with in situ measurements. J. Geophys. Res. Biogeosci. 111, G04017. https://doi.org/10.1029/2006JG000217.

Ziello, C., Sparks, T.H., Estrella, N., Belmonte, J., Bergmann, K.C., Bucher, E., et al., 2012. Changes to airborne pollen counts across Europe. PLoS One 7, e34076. https://doi.org/10.1371/journal.pone.0034076.

Ziska, L., Knowlton, K., Rogers, C., Dalan, D., Tierney, N., Elder, M.A., et al., 2011. Recent warming by latitude associated with increased length of ragweed pollen season in central North America. Proc. Natl. Acad. Sci. U. S. A. 108:4248–4251. https://doi.org/10.1073/pnas.1014107108.